

Supplementary Information

Doping Effect on the Structure and Properties of Eight-Electron Silver Nanoclusters

Yu-Jie Zhong,^a Jian-Hong Liao,^a Tzu-Hao Chiu,^a Franck Gam,^b Samia Kahlal,^b
Jean-Yves Saillard,^{*b} C. W. Liu^{*a}

^a Department of Chemistry, National Dong Hwa University, Hualien 974301, Taiwan (Republic of China). E-mail: chenwei@mail.ndhu.edu.tw; <http://faculty.ndhu.edu.tw/~cwl/index.htm>

^b Univ Rennes, CNRS, ISCR-UMR 6226, F-35000 Rennes, France.

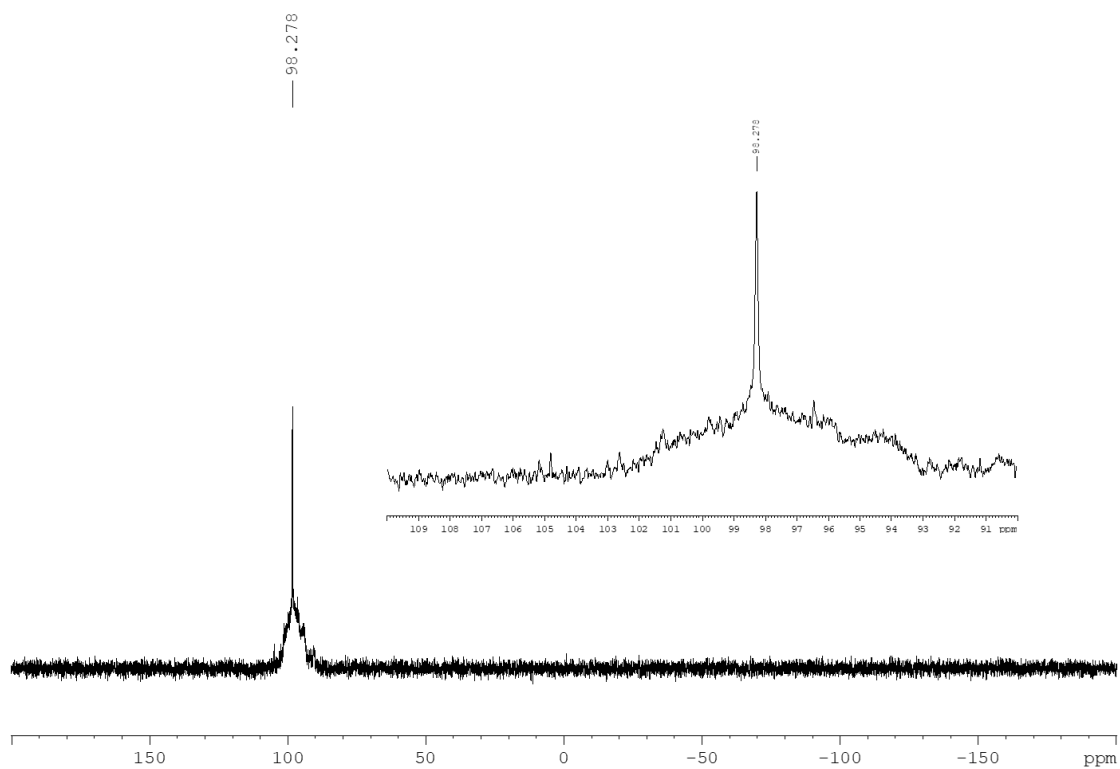


FIG. S1. The $^{31}\text{P}\{^1\text{H}\}$ NMR (CDCl_3) spectrum of **1**.

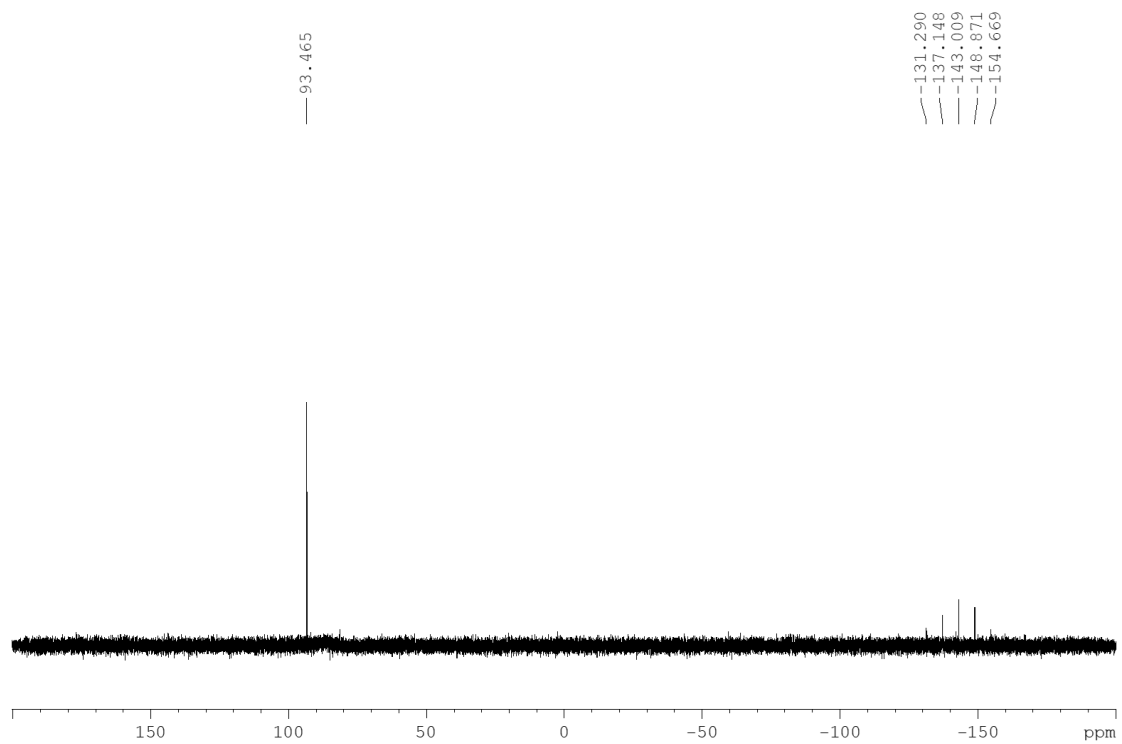


FIG. S2. The $^{31}\text{P}\{^1\text{H}\}$ NMR (CDCl_3) spectrum of **2**.

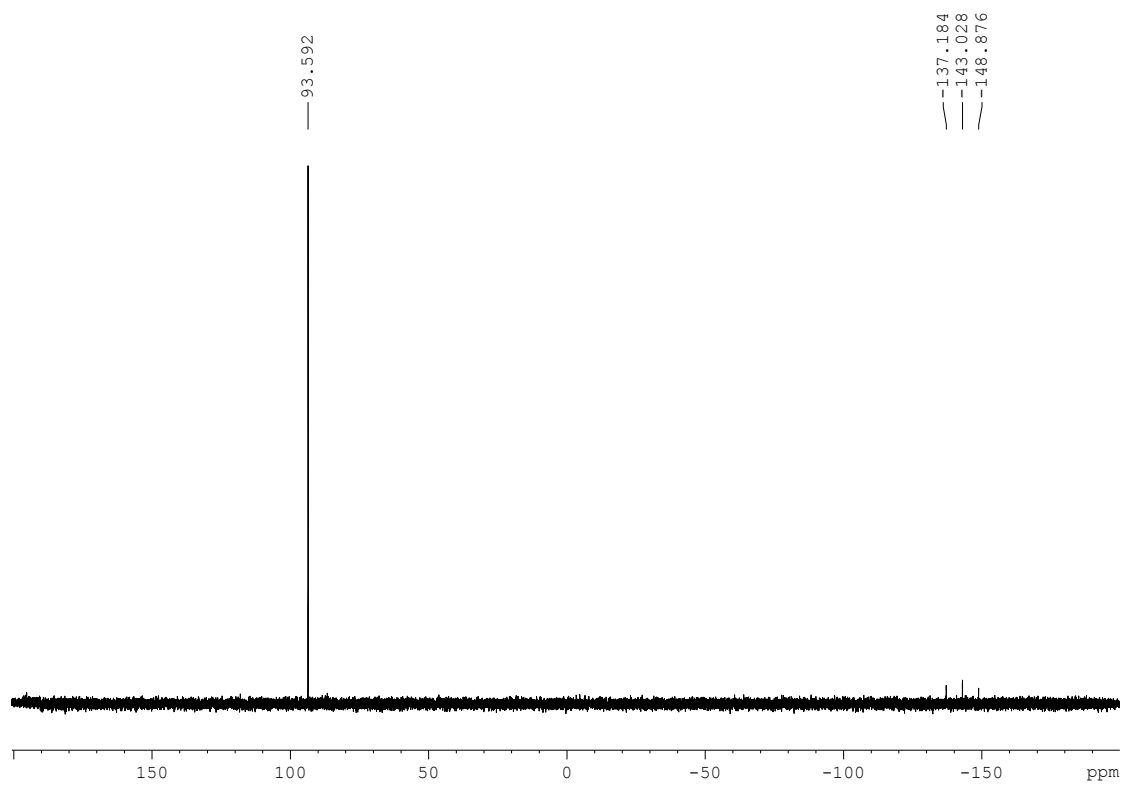


FIG. S3. The $^{31}\text{P}\{^1\text{H}\}$ NMR (CDCl_3) spectrum of **3**.

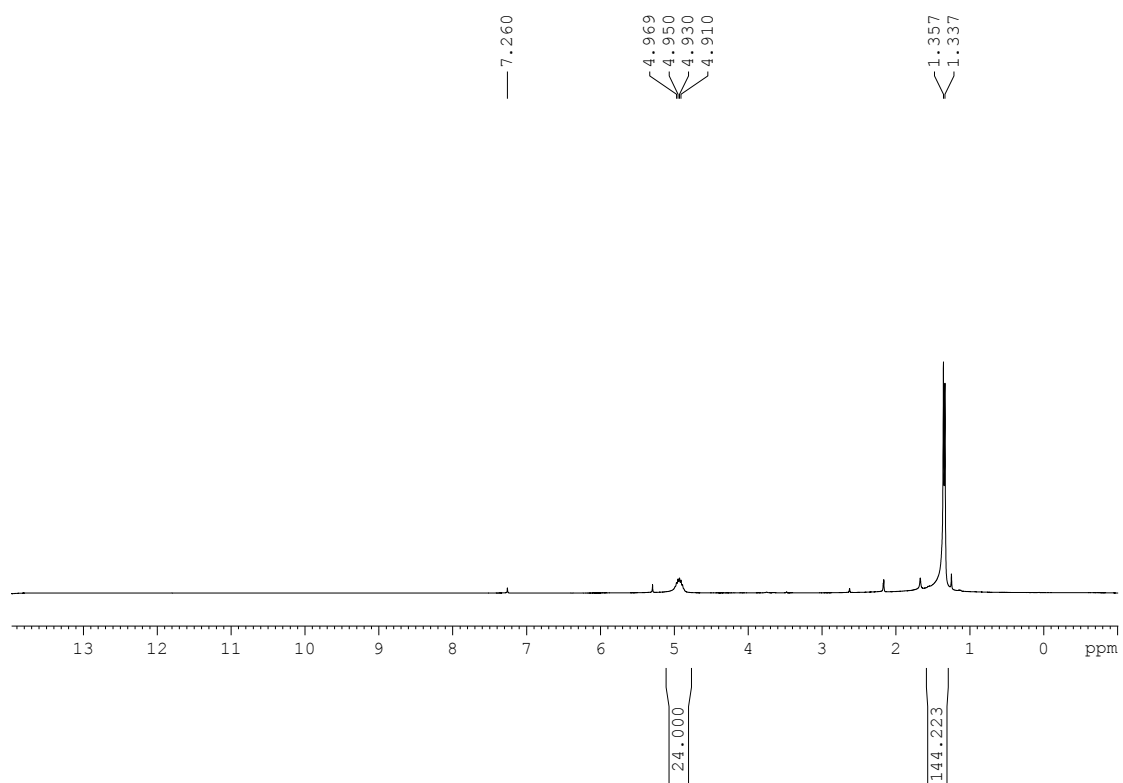


FIG. S4. The ^1H NMR (CDCl_3) spectrum of **1**.

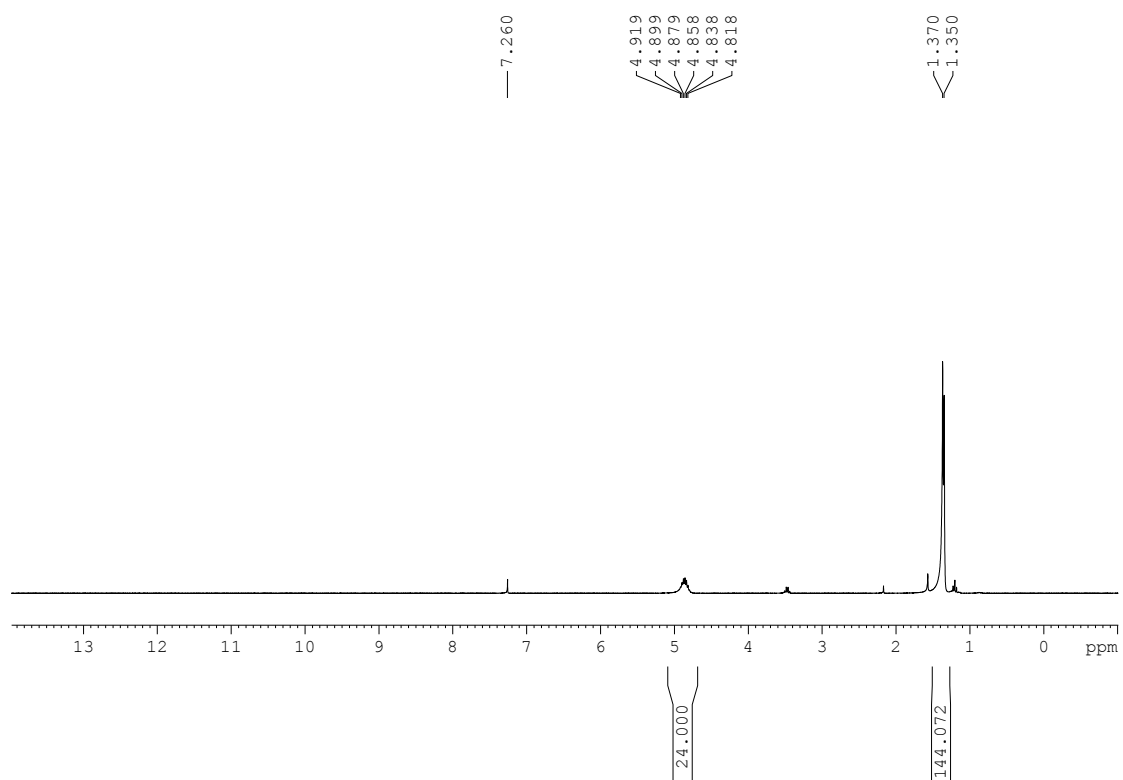


FIG. S5. The ^1H NMR (CDCl_3) spectrum of **2**.

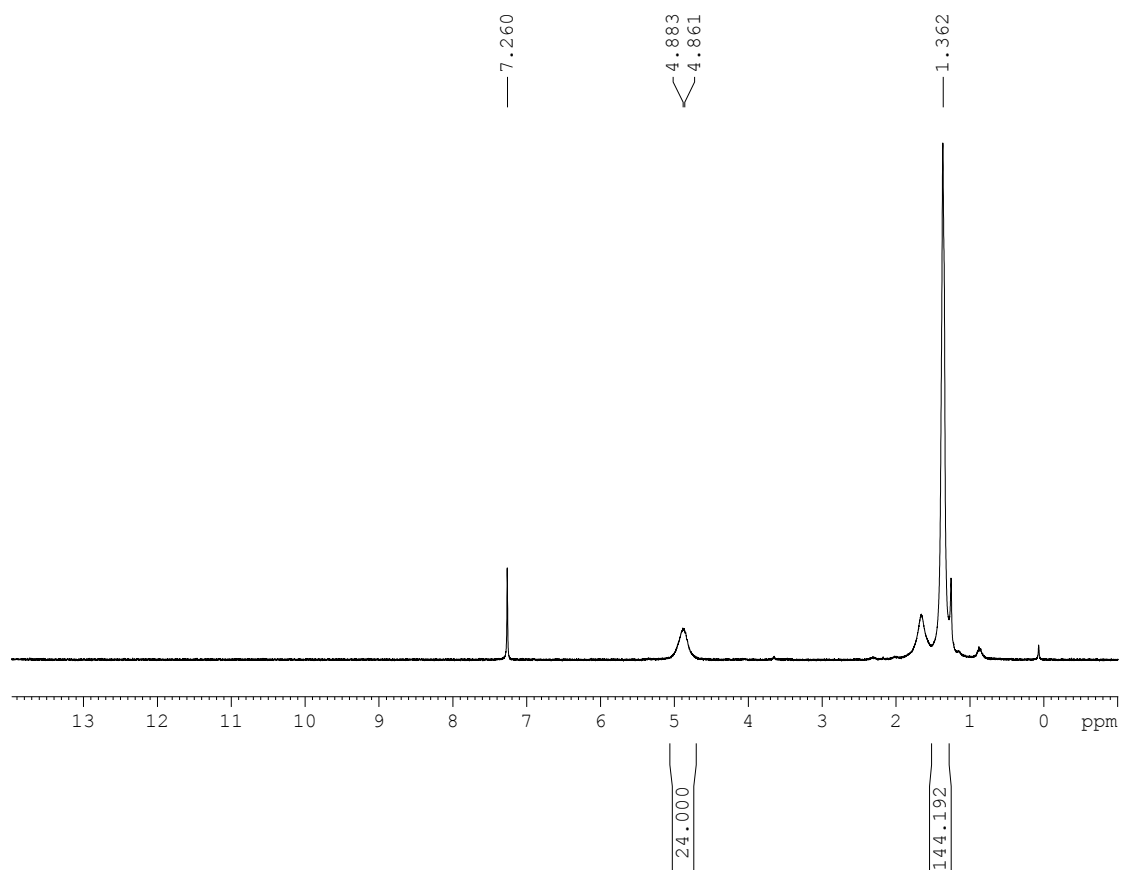


FIG. S5. The ^1H NMR (CDCl_3) spectrum of **3**.

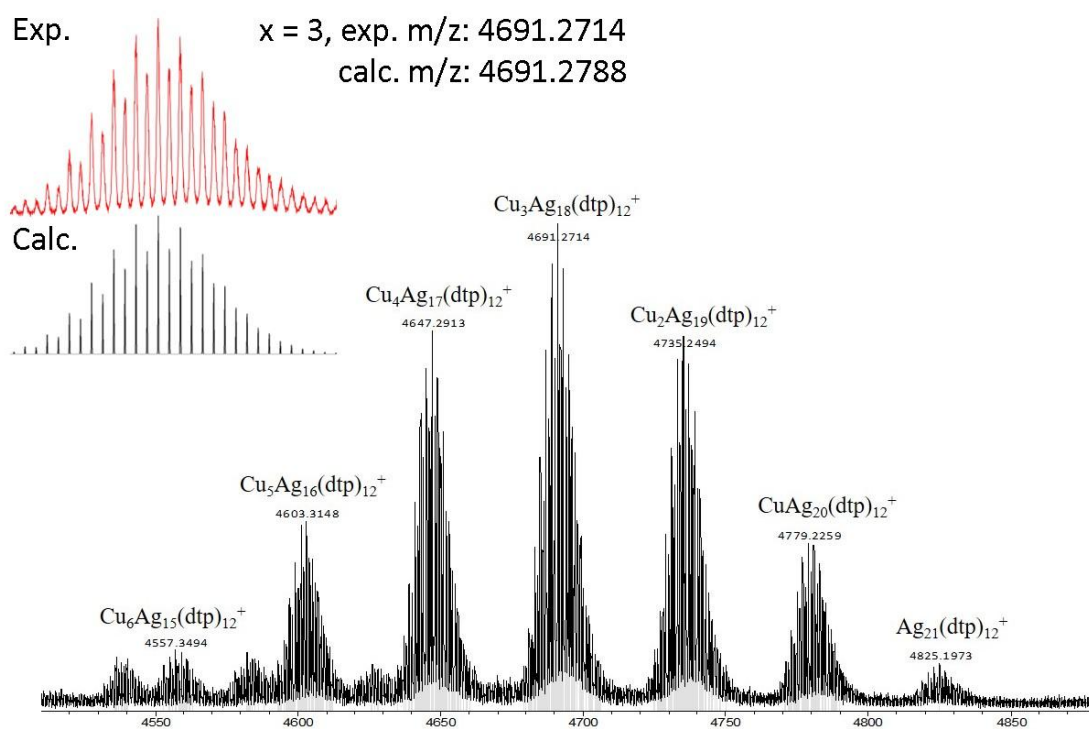


FIG. S7. ESI-MS spectrum of **2**. The distribution of molecular ion peaks is corresponding to $[\text{Cu}_x\text{Ag}_{21-x}\{\text{S}_2\text{P}(\text{O}^i\text{Pr})_2\}_{12}]^+$ ($x = 0-6$).

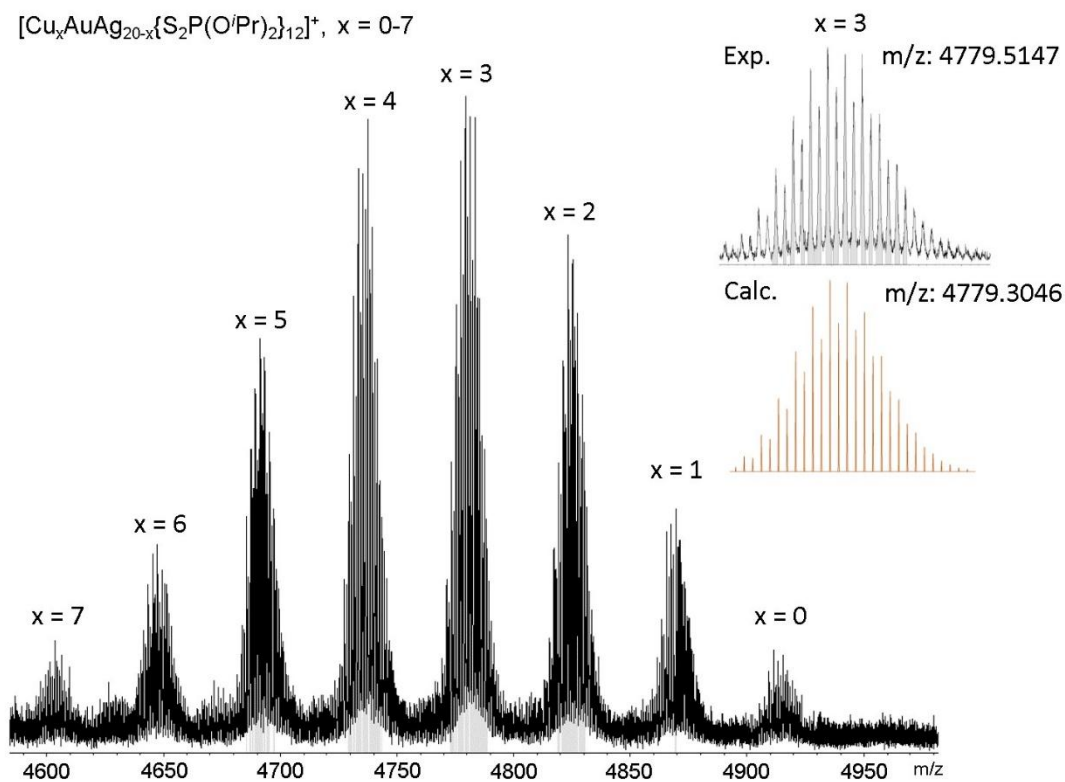


FIG. S8. ESI-MS spectrum of **3**. The distribution of molecular ion peaks is corresponding to $[\text{Cu}_x\text{AuAg}_{20-x}\{\text{S}_2\text{P}(\text{O}^i\text{Pr})_2\}_{12}]^+$ ($x = 0-7$).

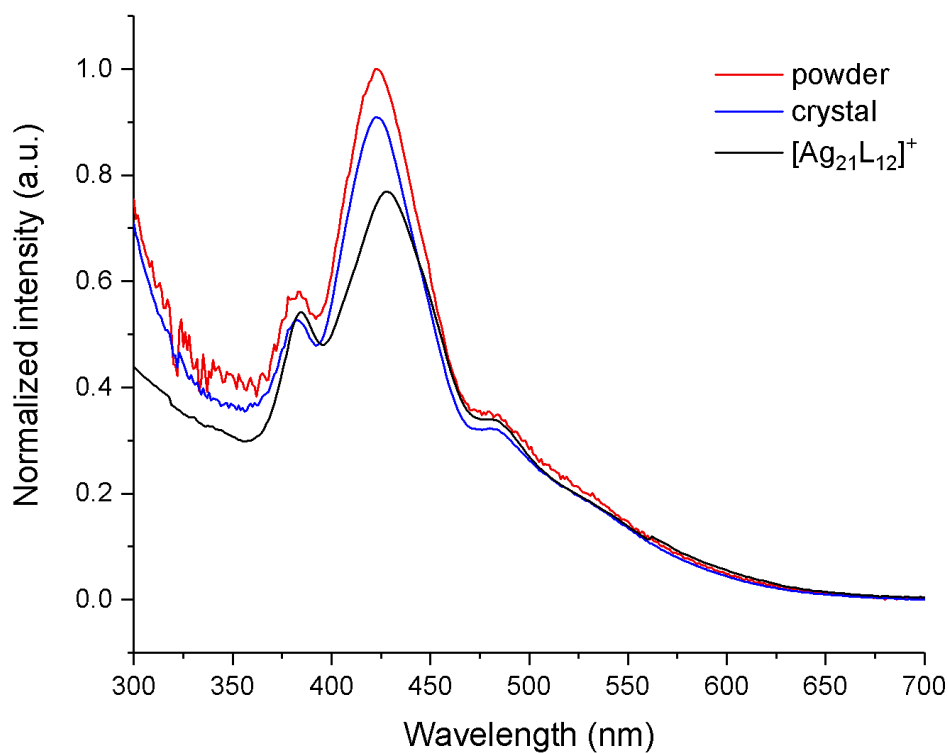


FIG. S9. The absorption spectra of **2** in powder (ref line), crystal (blue line), and $[\text{Ag}_{21}\{\text{S}_2\text{P}(\text{O}^i\text{Pr})_2\}_{12}]^+$ (black line) in 2-MeTHF.

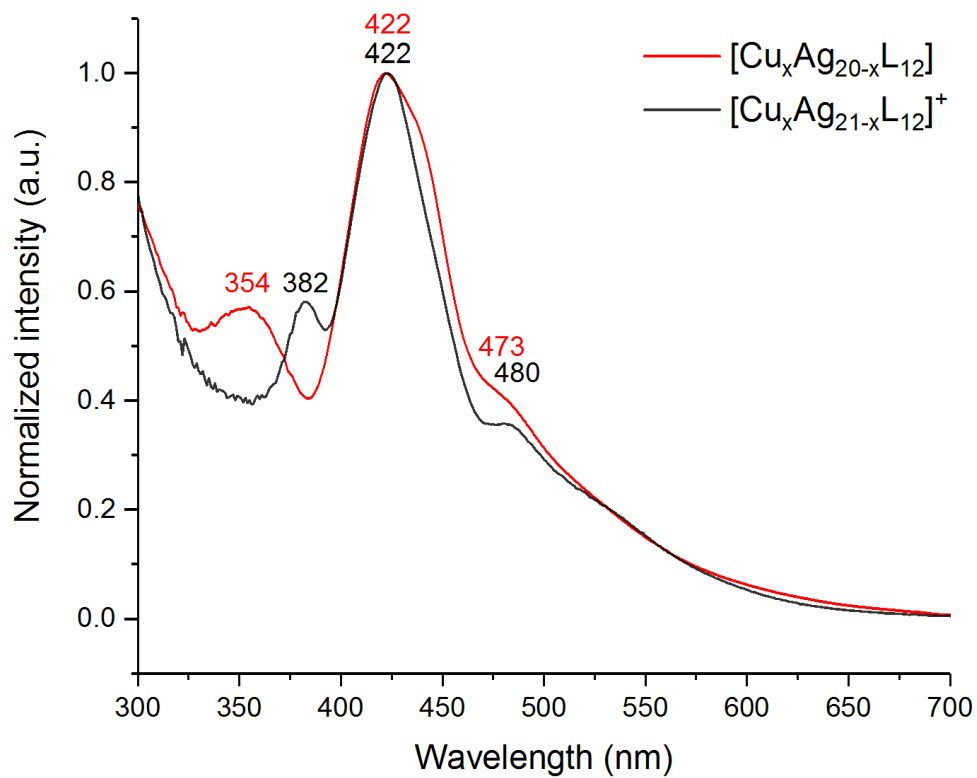


FIG. S10. The absorption spectrum of **1** (red line) and **2** (black line) in 2-MeTHF.

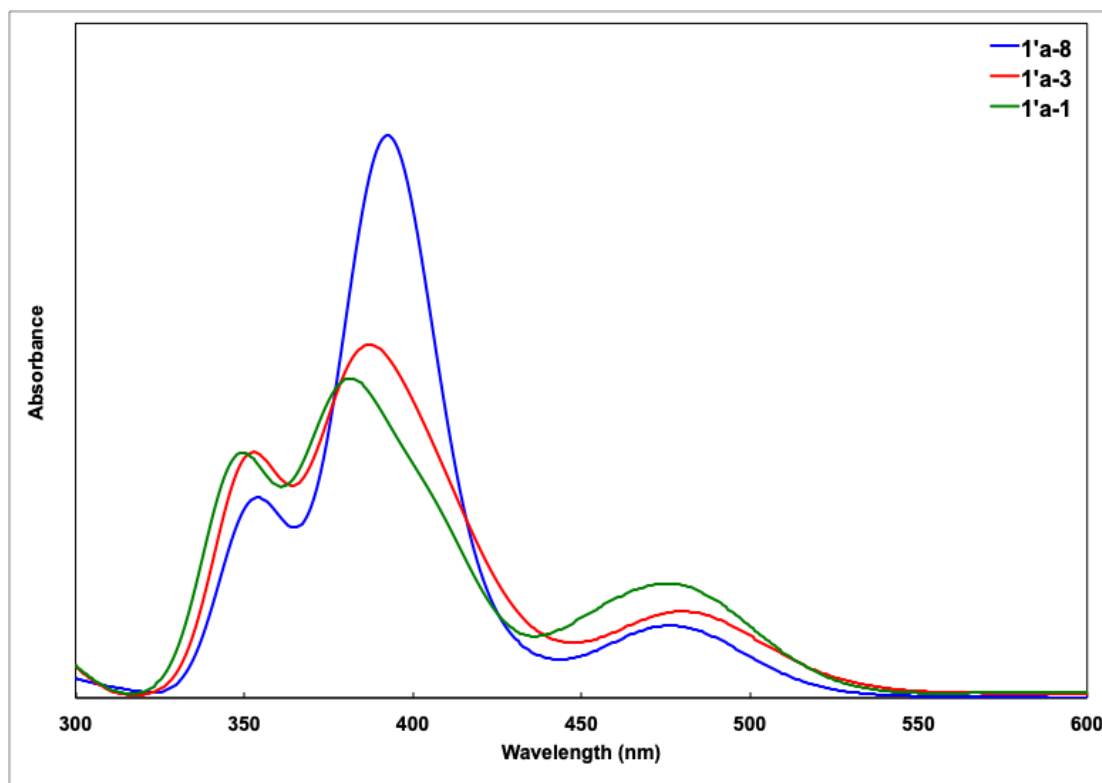


FIG. S11. The TD-DFT-simulated absorption spectra of a selection of positional isomers of **1a'** (see main text).

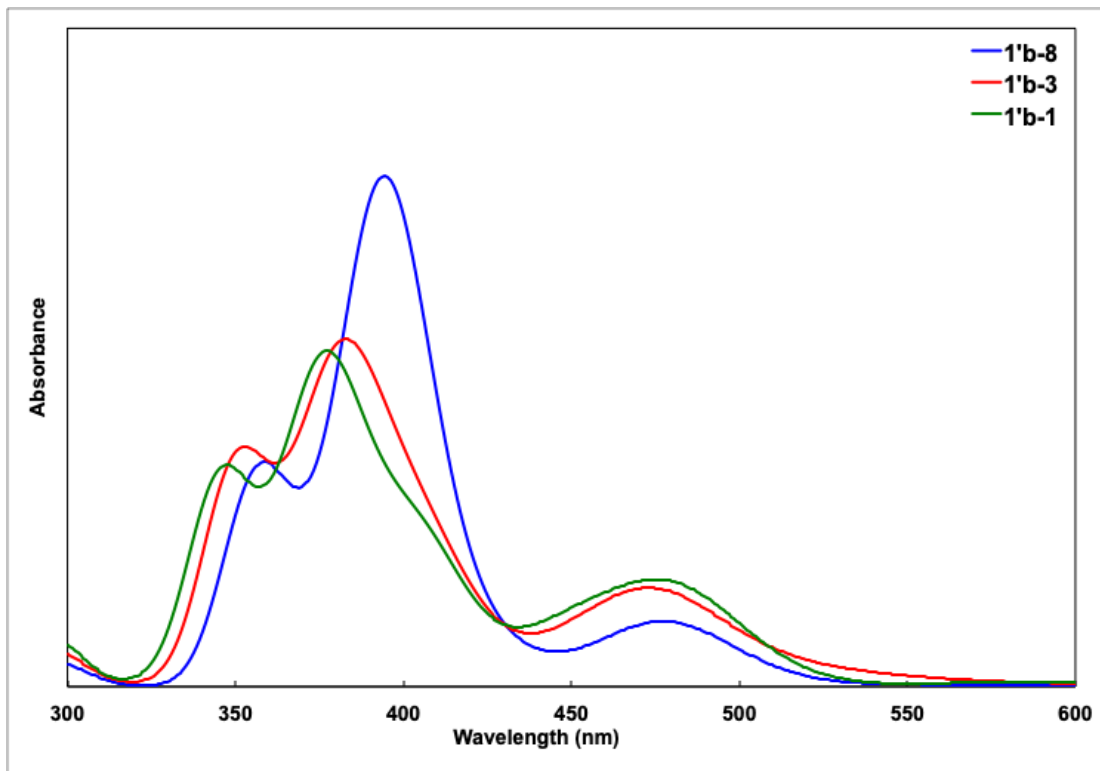


FIG. S12. The TD-DFT-simulated absorption spectra of a selection of positional isomers of **1b'** (see main text).

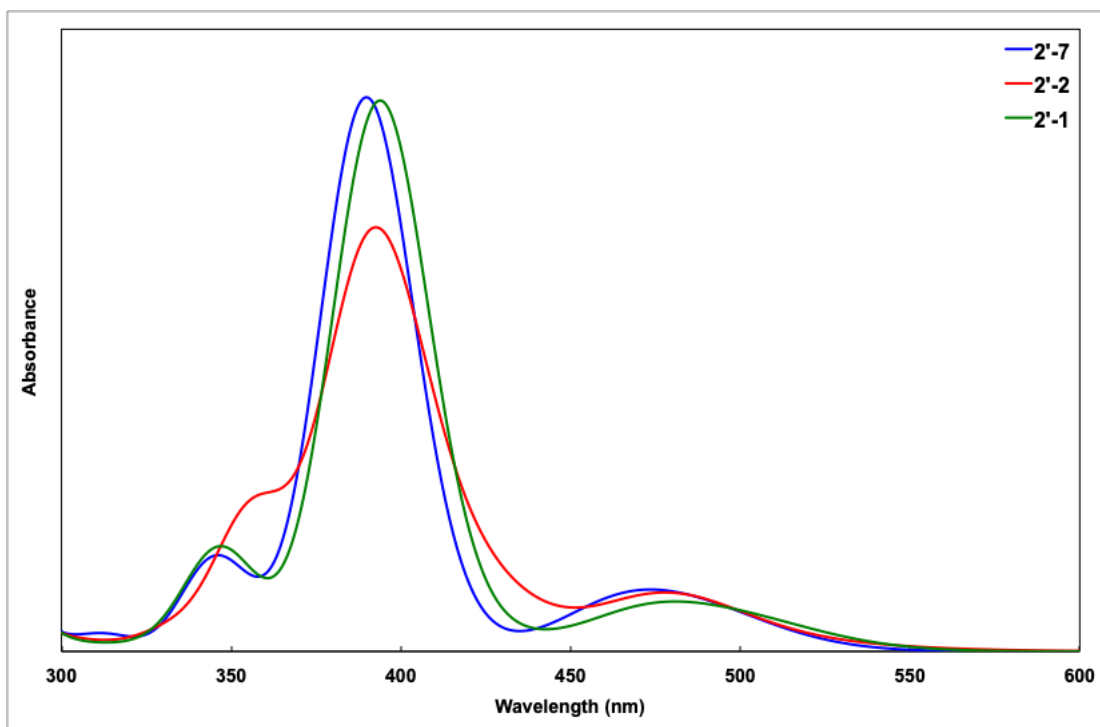


FIG. S13. The TD-DFT-simulated absorption spectra of a selection of positional isomers of **2'** (see main text).

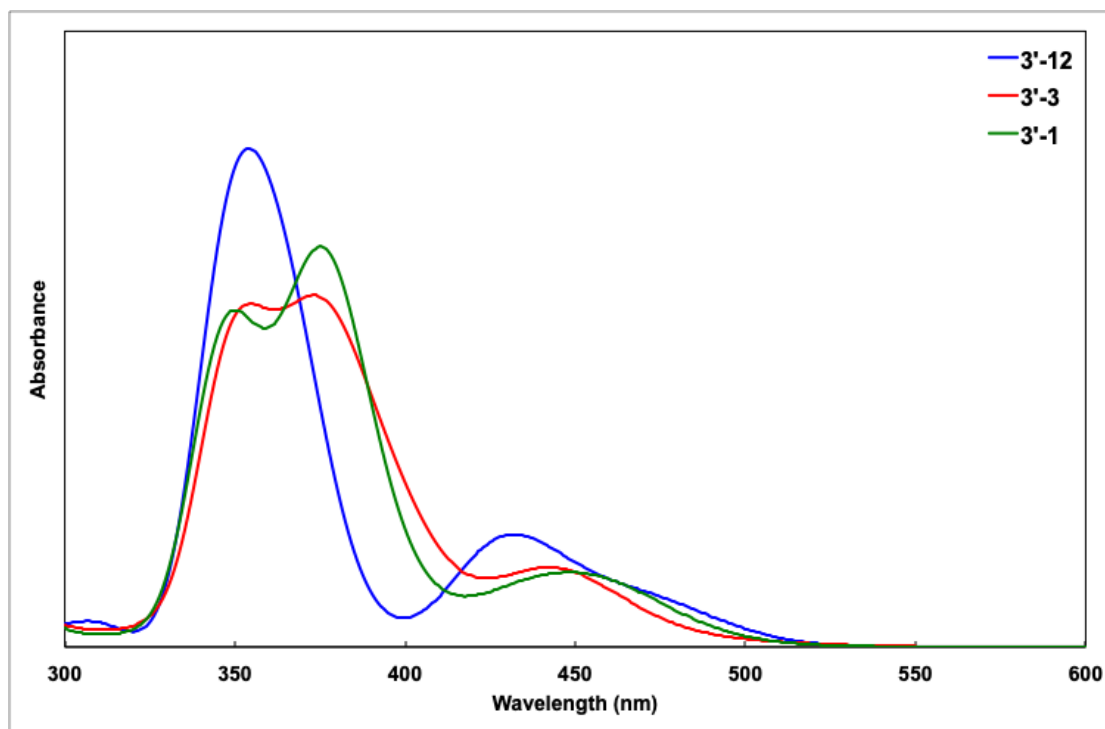


FIG. S14. The TD-DFT-simulated absorption spectra of a selection of positional isomers of **3'** (see main text).

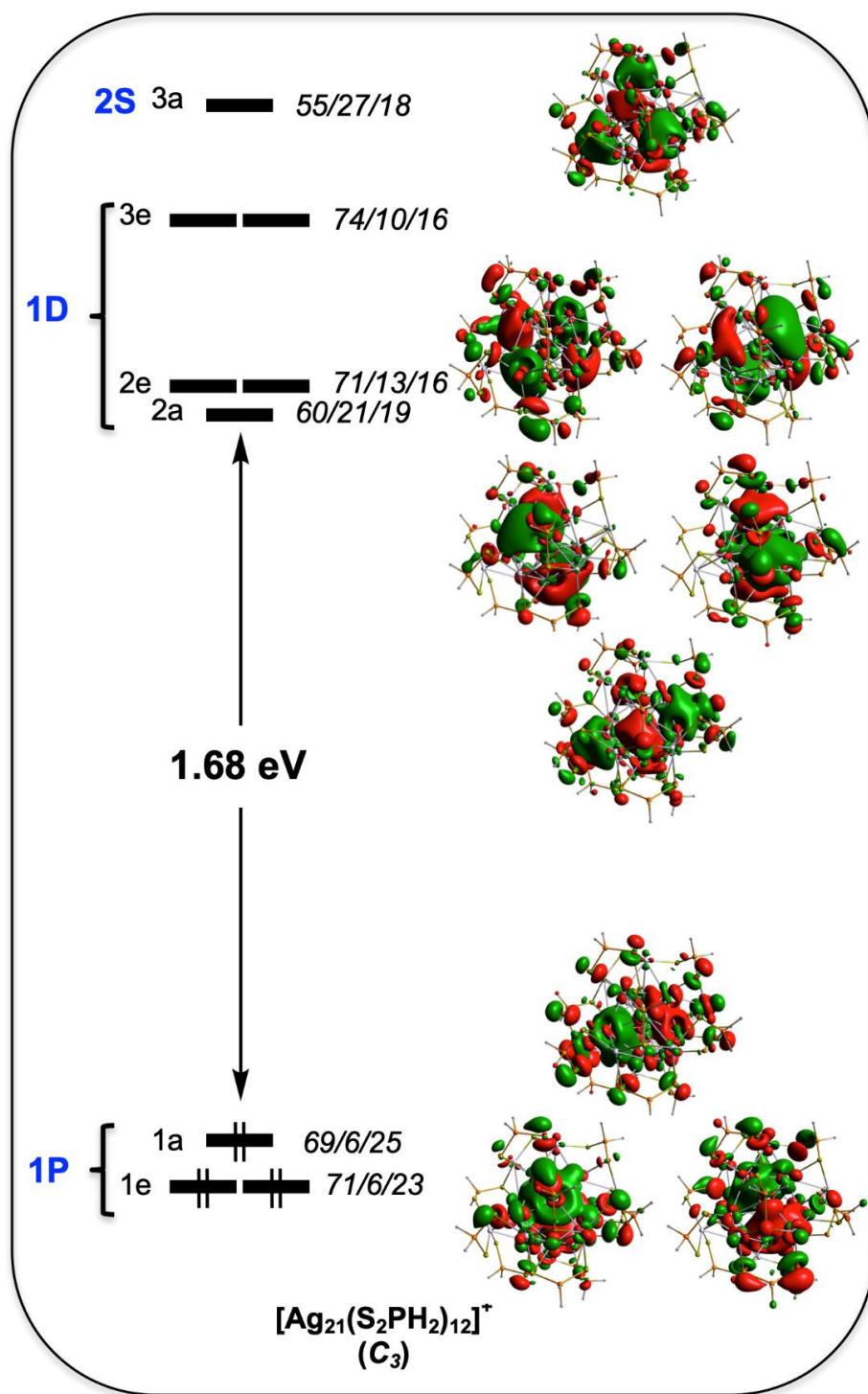


FIG. S15. Frontier Kohn-Sham MO diagram of the homometallic $[\text{Ag}_{21}(\text{S}_2\text{PH}_2)_{12}]^+$ model of C_3 symmetry. The MO localizations are given in % as $\text{Ag}_{13}(\text{icosahedron})/\text{Ag}_8(\text{caps})/\text{ligands}$.

TABLE SI. UV-vis absorption data of M_{20} and M_{21} nanoclusters.

M_{20} nanoclusters	UV-vis (λ , nm; ϵ , $M^{-1}cm^{-1}$)
$[Ag_{20}\{S_2P(O^iPr)_2\}_{12}]^{[a]}$	354 (4400), 422 (7700), 473 (3300)
$[Cu_xAg_{20-x}\{S_2P(O^iPr)_2\}_{12}]$ (1 , powder)	354 (4000), 422 (6100), 473 (2600)
$[Cu_3Ag_{17}\{S_2P(O^iPr)_2\}_{12}]_{0.5}[Cu_4Ag_{16}\{S_2P(O^iPr)_2\}_{12}]_{0.5}$ (1a) _{0.5} (1b) _{0.5} , crystal)	355 (4000), 422 (6100), 473 (2600)
M_{21} nanoclusters	
$[Ag_{21}\{S_2P(O^iPr)_2\}_{12}]PF_6^{[b]}$	385 (4900), 428 (6900), 480 (3000)
$[Cu_xAg_{21-x}\{S_2P(O^iPr)_2\}_{12}]PF_6$ (2 , powder)	382 (3900), 422 (5600), 480 (2400)
$[Cu_4Ag_{17}\{S_2P(O^iPr)_2\}_{12}]PF_6$ (2 , crystal)	382 (3900), 422 (5600), 480 (2400)
$[AuCu_xAg_{20-x}\{S_2P(O^iPr)_2\}_{12}]PF_6$ (3)	373 (4100), 413 (4700), 464 (2100)

^[a] Chem. Eur. J. **22**, 9943-9947 (2016). ^[b] Angew. Chem. Int. Ed. **54**, 3702-3706 (2015).

Table SII. Selected crystallographic data of [1a]_{0.5}[1b]_{0.5} and 2.

Compound	[Cu ₃ Ag ₁₇ {S ₂ P(O ⁱ Pr) ₂ } ₁₂] _{0.5} -[Cu ₄ Ag ₁₆ {S ₂ P(O ⁱ Pr) ₂ } ₁₂] _{0.5} [1a] _{0.5} [1b] _{0.5}	[Cu ₄ Ag ₁₇ {S ₂ P(O ⁱ Pr) ₂ } ₁₂]PF ₆ (2)
CCDC Number	2073787	2057371
Chemical formula	C ₁₄₄ H ₃₃₆ Ag ₃₃ Cu ₇ O ₄₈ P ₂₄ S ₄₈	C ₇₂ H ₁₆₈ Ag ₁₇ Cu ₄ F ₆ O ₂₄ P ₁₃ S ₂₄
Formula weight	9122.76	4792.05
Wavelength, Å	0.71073	0.71073
Crystal System	Monoclinic	Monoclinic
Space group	<i>P</i> 2 ₁ / <i>n</i>	<i>P</i> 2 ₁ / <i>n</i>
a, Å	16.7730(18)	16.8518(4)
b, Å	30.745(3)	30.8520(7)
c, Å	29.873(3)	30.5757(7)
α, deg.	90	90
β, deg.	94.371(2)	97.1300(7)
γ, deg.	90	90
V, Å ³	15360(3)	15773.7(6)
Z	4	4
Temperature, K	100(2)	150(2)
ρ _{calcd} , g/cm ³	1.972	2.018
μ, mm ⁻¹	3.023	3.088
θ _{max} , deg.	25.165	24.999
Completeness, %	99.3	99.9
Reflection collected / unique	80382 / 27352 [<i>R</i> _{int} = 0.0698]	93791 / 27744 [<i>R</i> _{int} = 0.0471]
Restraints / parameters	432 / 1417	529 / 1516
^a <i>R</i> 1, ^b <i>wR</i> 2 [<i>I</i> > 2σ(<i>I</i>)]	0.0668, 0.1310	0.0504, 0.1202
^a <i>R</i> 1, ^b <i>wR</i> 2 (all data)	0.0907, 0.1413	0.0739, 0.1345
GOF	1.127	1.087
Largest diff. peak and hole, e/Å ³	1.780 and -1.623	2.419 and -0.982

$$^a R1 = \frac{\sum ||F_o| - |F_c||}{\sum |F_o|} \quad ^b wR2 = \left\{ \frac{\sum [w(F_o^2 - F_c^2)^2]}{\sum [w(F_o^2)^2]} \right\}^{1/2}.$$